Dynamic Target Distribution Estimation for Source-Free Open-Set Domain Adaptation

Zhiqi Yu[1], Zhichao Liao[1], Jingjing Li[1*], Zhi Chen[2], Lei Zhu[3]

[1]University of Electronic Science and Technology of China (UESTC)
[2]School of Electrical Engineering and Computer Science, University of Queensland
[3]School of Electronic and Information Engineering, Tongji University
{zhiqiyu777,liaozhichao.light}@gmail.com, lijin117@yeah.net, zhi.chen@uq.edu.au, leizhu0608@gmail.com

Abstract

Unsupervised domain adaptation (UDA) has emerged as a promising technique for transferring knowledge from a labeled domain to an unlabeled domain. However, existing UDA methods are severely constrained by data privacy and semantic inconsistencies. To alleviate these limitations, this work challenges the Source-Free Open-Set Domain Adaptation (SF-OSDA), where the pre-trained source model is directly leveraged on the open target domain for adaptation. For this purpose, we introduce the novel Dynamic Target Distribution Estimation (DTDE) method, which effectively performs known classification and unknown separation through self-supervised learning with prototypes. To construct known prototypes, a self-adaptive sampling strategy is employed to consider the category disparity. For unknown prototypes, we utilize a self-splitting and excluding principle to bypass the unknown semantics problem. Specifically, self-splitting is to evaluate the overall clustering distribution of the target domain. By excluding clusters resembling known prototypes, the remaining cluster centroids can serve as unknown prototypes. The superiority of our approach is validated across multiple benchmarks. Remarkably, DTDE outperforms the best competitor by 7.6% on the VisDA dataset.

Introduction

Deep neural networks have significantly influenced this era, but the substantial volume of annotated data required for supervised training can result in expensive labor costs. To alleviate this issue, Unsupervised Domain Adaptation (UDA) (Tzeng et al. 2017; Ganin and Lempitsky 2015) is proposed to transfer knowledge from one labeled source domain to another unlabeled target domain. However, existing UDA methods (Kang et al. 2019; Hoffman et al. 2018; Yu et al. 2023; Bucci et al. 2021; Achituve, Maron, and Chechik 2021) are severely constrained in the real open world. Firstly, UDA requires simultaneous access to source and target domain data during the training process, which can potentially raise privacy concerns (Liang, Hu, and Feng 2020; Xia, Zhao, and Ding 2021) about the source data. Moreover, in the open world, the target domain probably contains unknown categories that have not appeared in the source domain. UDA mostly assumes that the source and target domains share the same label space, so all the unknown samples will be misclassified into known categories. This is not practical in reality as the identification of unknown samples is also critically important.

To overcome above limitations of UDA, it is necessary to explore how to directly transfer the model pre-trained on the source domain to the open target domain. We refer to this problem as the Source-Free Open-Set Domain Adaptation (SF-OSDA) setting. Previous Open-Set Domain Adaptation (OSDA) works (Panareda Busto and Gall 2017; Saito et al. 2018; Pan et al. 2020; Zhong et al. 2021) mostly utilize the labeled data of source domain to evaluate the distribution of known samples and simulate the potential distributions of unknown samples, thereby training the model to separate known and unknown samples with these distributions. This training strategy is not feasible in SF-OSDA, where the source domain data is not accessible. Therefore, the primary challenge of SF-OSDA lies in identifying the typical distribution of known and unknown samples.

In this work, we propose a simple yet effective SF-OSDA method primarily based on the Dynamic Target Distribution Estimation (DTDE). In DTDE, the distribution of the target domain is utilized to construct known and unknown prototypes. For known prototypes, we adopt a self-adaptive sampling strategy to build a flexible support-sample set that considers the category disparity within the dataset. To construct unknown prototypes, we propose to use the clustering distribution to represent the distribution of unknown samples with a self-splitting and excluding principle. Specifically, self-splitting is to evaluate the overall clustering distributions based on the intra-cluster compactness and inter-cluster separability. Consequently, by excluding the clustering centroids resembling known prototypes, the remaining centroids can serve as unknown prototypes. The obtained known and unknown prototypes can be used to pseudo-label the target data for self-supervised training. Additionally, a class-aware K-Nearest Neighbors (KNN) alignment is complemented to avoid incorrect pseudo-labels during the training process, especially on the challenging categories. The contribution of our work can be summarized as:

1. We challenge a practical but difficult source-free open-set domain adaptation setting, directly transferring the pre-trained source model to the open target domain for

*Corresponding author
Copyright © 2025, Association for the Advancement of Artificial Intelligence (www.aaai.org). All rights reserved.

adaptation, no longer relying on source data.

2. We propose a self-splitting mechanism to evaluate the clustering distribution over the target domain. This mechanism also allows for a reliable and efficient estimation of the total category number on the unknown domain.
3. Based on the dynamic target distribution estimation, we propose a simple yet effective source-free OSDA method termed as DTDE. Without access to source data, the performance of DTDE on multiple mainstream benchmarks reaches and even surpasses that of the state-of-the-art traditional OSDA methods.

Related Work

Closed-set domain adaptation (CSDA). CSDA primarily considers the distribution shift between the source domain and the target domain data with the shared label space. Existing methods can be broadly categorized into three main types: metric based, adversarial based and self-supervision based. Metric-based methods (Long et al. 2015, 2017; Kang et al. 2019) mitigate domain shift by utilizing specific metrics to align the feature distribution across domains. Adversarial-based methods (Tzeng et al. 2017; Ganin et al. 2016; Hoffman et al. 2018; Yu et al. 2023, 2022) seek to extract domain-invariant features in an adversarial fashion inspired by GAN (Goodfellow et al. 2014). Self-supervision based methods (Bucci et al. 2021; Achituve, Maron, and Chechik 2021; Gu, Sun, and Xu 2020) typically involve assigning pseudo-labels to the target domain data and then self-updating the model based on these pseudo-labels. Currently, souce-free domain adaptation (SFDA) (Liang, Hu, and Feng 2020; Xia, Zhao, and Ding 2021; Liu, Zhang, and Wang 2021; Yang et al. 2021) has garnered widespread attention. SFDA exclusively employs a pre-trained source model for target domain adaptation, effectively addressing privacy concerns associated with source data. Most previous works of SFDA are built on the closed-set assumption and are not suitable for the open-set setting.

Open-set domain adaptation (OSDA). OSDA is a more challenging setting compared to CSDA, which involves simultaneously classifying known samples and identifying unknown samples in the open target domain. Some approaches achieve the separation of known and unknown samples in the target domain through adversarial learning (Jang et al. 2022; Saito et al. 2018) or open-set classifiers (Liu et al. 2019; Bucci, Loghmani, and Tommasi 2020). Other methods utilize pseudo-labeling (Luo et al. 2020; Wang, Meng, and Breckon 2022) or adversarial training (Liu et al. 2019; Shermin et al. 2020) to align cross-domain data distributions. The former research line requires the introduction of additional structures for specific training on the source domain, while the latter research line necessitates access to source domain data.

Universal domain adaptation (UniDA). UniDA can be regarded as a superset of OSDA, in which both the source-private categories and the target-private categories coexist. DANCE (Saito et al. 2020) employs self-supervision techniques to promote alignment between the target samples and their neighbors. OVANet (Saito and Saenko 2021) uses multiple binary classifiers with a one-vs-all strategy to distinguish known and unknown samples. GLC (Qu et al. 2023) is the first source-free UniDA method and designed a one-vs-all global clustering algorithm for unknown sample identification. However, GLC requires performing a clustering operation on each class at each iteration, which is quite inefficient. Recently, LEAD (Qu et al. 2024) utilizes feature decomposition of known and unknown components to enhance the performance of the UniDA methods.

Method

Problem Formulation

In terms of the OSDA setting, there is usually a labeled source domain dataset $\mathcal{D}_s = \{(\boldsymbol{x}_i^s, y_i^s)\}_{i=1}^{N_s} \sim p_s$ as well as a related unlabeled target domain dataset $\mathcal{D}_t = \{\boldsymbol{x}_i^t\}_{i=1}^{N_t} \sim p_t$. p_s and p_t represent the marginal distributions of the source domain and target domain, respectively. Note that the label space of the source domain $\mathcal{C}_s$ is a true subset of the label space of the target domain $\mathcal{C}_t$, i.e., $\mathcal{C}_s \subsetneq \mathcal{C}_t$. This means that OSDA needs to deal with both distributional shift where $p_s \neq p_t$ and category shift where $\mathcal{C}_s \neq \mathcal{C}_t$. The goal of OSDA is to achieve the classification of known samples and the identification of unknown samples. This task can be viewed as a $|\mathcal{C}_s + 1|$ way classification problem, where the first $|\mathcal{C}_s|$ classes are known categories, and the last way is for identifying unknown samples. In particular, in this work we challenge the source-free OSDA setting where the pre-trained source model is directly used for target domain adaptation without source domain data. Furthermore, we also evaluate DTDE on the more challenging UniDA scenario, where there are certain private categories in the source domain that do not appear in the target domain.

Framework Overview

Our entire algorithm framework can be divided into three stages as shown in Figure 1. In the first stage, unlike previous OSDA methods that require specific open-set classifiers and additional training on the source domain, we adopt the same supervised training strategy in closed-set SFDA (Liang, Hu, and Feng 2020; Ding et al. 2022; Yang et al. 2021) to facilitate model reusability and transferability. In the second stage, a self-adaptive sampling strategy is used to construct the semantic prototypes of known categories. For unknown prototypes, a clustering self-splitting mechanism is first proposed to evaluate the target clustering distribution. Based on this, the unknown prototypes can be obtained by excluding all clustering distributions resembling the known prototype. Subsequently, the prototypes are utilized for self-supervised learning and the class-aware KNN alignment is employed to avoid incorrect pseudo-labels. In the third stage, the model is used for inference. The target samples within the uncertainty threshold are identified as known samples of the maximum probability category, while samples beyond the uncertainty threshold are identified as unknown samples.

Pre-training on Source Data

SFDA aims to directly transfer the pre-trained source model to the target domain without accessing the source domain

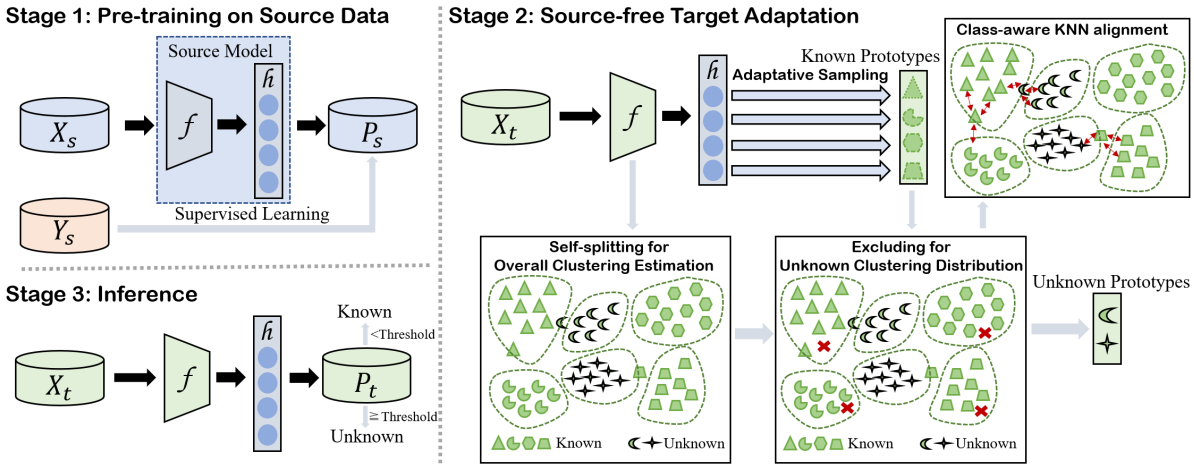

Figure 1: Illustration of our proposed DTDE. *Stage-1*: Perform supervised learning on the model output P_s with the source dataset X_s and the corresponding label Y_s. The source model consists of a feature extractor f and a closed-set classifier h. *Stage-2*: The model is initialized with the source model and only the feature extractor is subsequently updated. Initially, a support-sample set is built through the self-adaptive sampling strategy to construct the known prototypes. Next, a self-splitting mechanism is used to evaluate the target clustering distribution. By excluding clustering distributions similar to the known prototypes, the unknown prototypes are obtained. Finally, the class-aware KNN alignment is applied to avoid incorrect pseudo-labels. *Stage-3*: Inference to target data and identify unknown samples through the uncertainty threshold.

data, thus preserving personal privacy and enhancing transfer efficiency. To introduce the source-free setting into OSDA, a common model structure and source training strategy are required. However, most existing OSDA methods require a method-specific open-set classifier and additional training on the source domain. These differentiated source training strategies can severely compromise the generalizability of SF-OSDA. In this work, we utilize the same model structure and training strategy in SFDA (Liang, Hu, and Feng 2020; Yang et al. 2021; Ding et al. 2022), which can be formulated as follows:

$$\mathcal{L}_{src} = -\frac{1}{N_s}\sum_{i=1}^{N_s}\sum_{c=1}^{|\mathcal{C}_s|} y_i^s \log \delta_c(h(f(x_i^s))), \tag{1}$$

where the source model contains a feature extractor f and a closed-set classifier h, N_s is the number of samples in the source domain, y_i^s denotes the ground-truth label of source sample x_i^s, and $\delta_c(,)$ denotes the soft-max probability on c-th category. Since the classifier weights may contain known category semantics, the parameters of the classifier are fixed and only the feature extractors are updated for adaptation.

Source-free Target Adaptation

In this section, we start by constructing known and unknown prototypes through the distributions of known and unknown samples. Then the obtained prototypes are utilized for self-supervised learning. Finally, the class-aware KNN alignment is a complement to avoid incorrect pseudo-labels during training, especially on those challenging categories.

Self-adaptive Sampling Strategy for Known Prototypes. Since the semantics of known categories are implicit in the weights of the classifier, it is relatively easy to find the distributions of known samples. In other words, the high-confidence samples within a certain category are likely to be located within the distribution of that category. Therefore, we can choose these high-confidence samples to build a support-sample set to represent the distributions of the known categories. The size of the support-sample set is worth discussing here, because if the size is set to a fixed value, the effectiveness of the support-sample set will heavily depend on the data scale. In addition, there may exist class imbalance issues within the dataset. Inspired by self-paced learning (Jiang et al. 2014; Lu et al. 2023), we developed a self-adaptive sampling strategy:

$$\begin{cases} \mathcal{S}_c = \{\delta_c(h(f(x^t))) > \epsilon \cdot H_c\}, \\ \mathcal{P}_c^{kn} = \dfrac{\sum_{x^t \in \mathcal{S}_c} f(x^t)}{|\mathcal{S}_c|}, \end{cases} \tag{2}$$

where $\mathcal{S}_c$ indicates the support-sample set of the c-th known category, $\delta_c(h(f(x^t)))$ denotes the output probability of sample x^t in the c-th class, and H_c represents the maximum probability among all the target samples in the c-th category. The parameter $\epsilon \in (0, 1]$, controls the size of the support-sample set and exhibits robustness across datasets. Finally, taking the mean of the support-sample set yields the prototype of the c-th known category, i.e., $\mathcal{P}_c^{kn}$. Through our self-adaptive sampling strategy, it is flexible to obtain the appropriate support-sample sets based on the actual distributions of each category.

Clustering Distribution Estimation for Unknown Prototypes. In SF-OSDA, it's challenging to determine the distribution of unknown samples with the classifier's output

due to their unknown semantics. To bypass this problem, we novelly propose to use the clustering distributions in the target domain to represent the distributions of unknown samples. The motivation behind this is that the target domain data can form clear clusters even without aligning with the source classifier (Yang et al. 2021; Su et al. 2023). In particular, a self-splitting and excluding principle is adopted. Firstly, we evaluate the overall clustering distribution of the target domain through self-splitting. Furthermore, by excluding the clustering distributions that are similar to the known prototypes, the remaining distributions can serve as the distribution of unknown samples.

Step 1. Self-splitting for Overall Clustering Distribution: Assuming that the clustering distribution over the target domain can be accurately evaluated, the obtained clusters should exhibit strong intra-cluster compactness and inter-cluster separability. In other words, the disparity among samples within each cluster should be minimized, while the disparity among samples of different clusters should be maximized. This objective can be formalized as:

$$\arg\min_{K} \sum_{x_1,x_2 \in \Delta_0}^{\mathrm{F}(x_1)=\mathrm{F}(x_2)} \mathrm{Dis}(x_1,x_2) - (\lambda/K) \sum_{x_1,x_2 \in \Delta_0}^{\mathrm{F}(x_1)\neq\mathrm{F}(x_2)} \mathrm{Dis}(x_1,x_2), \quad (3)$$

where $\mathrm{Dis}(,)$ denotes the disparity function and $\Delta_0 = \{\mathcal{F}_1, ..., \mathcal{F}_K\}$ indicates that the target domain is now clustered into K clustering distributions. $\mathrm{F}(x_1) = \mathrm{F}(x_2)$ means that x_1 and x_2 belong to the same cluster and $\mathrm{F}(x_1) \neq \mathrm{F}(x_2)$ vice versa. The first term represents the compactness within the cluster, the second term represents the separability between clusters, and λ is the balancing parameter between the two terms. x_1, x_2 are features processed by the feature extractor.

To achieve this goal, we apply a greedy principle with the clustering self-splitting mechanism. Specifically, a small initial value is set for clustering in the target domain. Subsequently, we attempt to split each cluster into two sub-clusters, requiring that the clustering performance after splitting is superior to before. This process continues until all clusters no longer split. Given that it is now the turn for the K-th cluster to split, this process can be formulated as:

$$\begin{aligned} &\sum_{x_1,x_2 \in \Delta_1}^{\mathrm{F}(x_1)=\mathrm{F}(x_2)} \mathrm{Dis}(x_1,x_2) - (\lambda/K+1) \sum_{x_1,x_2 \in \Delta_1}^{\mathrm{F}(x_1)\neq\mathrm{F}(x_2)} \mathrm{Dis}(x_1,x_2) \leq \\ &\sum_{x_1,x_2 \in \Delta_0}^{\mathrm{F}(x_1)=\mathrm{F}(x_2)} \mathrm{Dis}(x_1,x_2) - (\lambda/K) \sum_{x_1,x_2 \in \Delta_0}^{\mathrm{F}(x_1)\neq\mathrm{F}(x_2)} \mathrm{Dis}(x_1,x_2), \end{aligned} \quad (4)$$

where $\mathcal{F}_K^1, \mathcal{F}_K^2$ denote the two sub-clusters obtained from the current split, and $\Delta_1 = \{\mathcal{F}_1, ..., \mathcal{F}_{K-1}, \mathcal{F}_K^1, \mathcal{F}_K^2\}$. The left and right sides of the equation represent the clustering performance before and after the split, respectively. The smaller value indicates the better clustering performance. In this paper, we employ the Jensen-Shannon (JS) divergence as the disparity function to measure the difference between two clusters. Kmeans clustering (MacQueen et al. 1967) is selected as the clustering technique due to its ease of implementation. To further reduce computational overhead, this process can be simplified as:

$$\frac{\lambda}{K(\lambda+K+1)} \frac{\sum_{i,j\in[K]}^{i\neq j} \mathrm{JS}(\mathcal{F}_i, \mathcal{F}_j)}{\mathrm{JS}(\mathcal{F}_K^1, \mathcal{F}_K^2)} \leq 1. \quad (5)$$

This equation means that if the above equation is less than 1, the current cluster will be split into two sub-clusters. The detailed proof can be found in the appendix. Suppose that the clustering distributions as $\{\mathcal{F}_1, \mathcal{F}_2, ..., \mathcal{F}_{M_t}\}$ is now obtained by the self-splitting mechanism. At this point, these clustering distributions are still semantically ambiguous. In the next section, we will use a excluding principle to find the distributions of unknown samples among these distributions.

Step 2. Excluding for Unknown Clustering Distribution: The clustering distributions in the target domain can represent either known samples or unknown samples. By excluding the clustering distributions similar to the known prototypes, we can use the remaining clustering distributions to represent unknown samples. As the clustering centroid is a strong representative of the clustering distribution, this strategy can be formulated as follows:

$$\begin{aligned} \mathcal{P}^{un} &= \{\mu_i\}_{i=1}^{M} - \{\mu_c^{kn}\}_{c=1}^{|\mathcal{C}_s|}, \\ \mu_c^{kn} &= \{\mu_i \mid \mu_i \in \{\mu_i\}_{i=1}^{M},\ \mathrm{Sim}(\mu_i, \mathcal{P}_c^{kn}) > \tau_c\}, \end{aligned} \quad (6)$$

where $\{\mu_i\}_{i=1}^{M}$ denotes the clustering centroids set. Here we have reclustered the target domain samples as $\{\mathcal{F}_1, \mathcal{F}_2, ..., \mathcal{F}_M\}$, where $M = M_t + |\mathcal{C}_s|$. This operation aims to retain a specific number of redundant clusters, considering the potential for multiple centroids to represent a prototype. $\mathrm{Sim}(,)$ denotes the similarity calculation function, and we employ cosine similarity. The similarity threshold τ_c is acquired by averaging the similarities among the top three most similar clusters within the i-th known class. τ_c serves to alleviate potential clustering algorithm errors, allowing us to exclude the most similar one or two centroids based on the actual situation of each known category.

Currently, all the prototypes $\mathcal{P} = \{\mathcal{P}^{kn}, \mathcal{P}^{un}\}$ have been constructed in the target domain. Based on these prototypes, pseudo-labels can be assigned to the target samples. For a target sample, calculate its cosine similarity with each prototype. If the most similar prototype belongs to a known category, the sample is identified as known and assigned the corresponding one-hot pseudo-label. Conversely, if this sample is most similar to one of the unknown prototypes, it will be identified as unknown and its pseudo-label will be a uniform distribution with a value of $(1/|\mathcal{C}_s|)$. With these pseudo-labels, we can use cross-entropy to perform self-supervised learning on the model as:

$$\mathcal{L}_{pse} = -\frac{1}{N_t} \sum_{i=1}^{N_t} \sum_{c=1}^{|\mathcal{C}_s|} \hat{p}_i \log \delta_c(h(f(x_i^t))), \quad (7)$$

where $\hat{p}_i$ denotes the pseudo-label of the sample x_i^t.

Class-aware K-nearest Neighbors Alignment. Although the pseudo-labels obtained through the prototypes can be used for self-supervised learning, incorrect pseudo-labels can cause error accumulation during the training process (Chen et al. 2019). An intuitive solution is to identify mislabeled samples and correct them based on the confidence of each sample's output. However, due to the model's overconfidence issue (Ma et al. 2022; Liu, Wang, and Long 2021), the model often generates many incorrect but low-confidence pseudo-labels for some challenging categories at the beginning, and the confidence of these pseudo-labels will unconditionally increase in the training process. Therefore, we designed a class-aware correction weight based on the overall confidence of each category:

$$\begin{aligned} A_c &= \frac{\sum_{i=1}^{N_t} I_{c_i} \cdot \delta_c(h(f(x_i^t)))}{\sum_{i=1}^{N_t} I_{c_i}}, \\ w_c &= |\mathcal{C}_s| \times \delta_c(\frac{A_{max} - A_c}{A_{max} \times t}), \end{aligned} \tag{8}$$

where I_c is the indicator matrix for the c-th class, $I_{c_i} = 1$ when the i-th sample is predicted to be the c-th class, otherwise $I_{c_i} = 0$. This allows A_c to represent the overall confidence coefficient of the c-th category. A_{max} represents the maximum value among all the known classes and t is a temperature parameter. Consequently, w_c serves as the correction weight for the c-th category, increasing as the overall confidence coefficient decreases due to challenging categories necessitating higher correction weights. Then we inject it to the K-Nearest Neighbors (KNN) alignment loss (Qu et al. 2023), so that when the sample is predicted as a challenging category, it will be given greater weight to offset the negative impact of incorrect pseudo labels. The class-aware KNN alignment loss can be formulated as:

$$\mathcal{L}_{ali} = -\frac{1}{N_t} \sum_{i=1}^{N_t} \sum_{c=1}^{|\mathcal{C}_s|} w_c(u_i \log \delta_c(h(f(x_i^t)))), \tag{9}$$

where u_i is the average output of the nearest several neighbors to sample x_i^t in the memory bank we maintained, and the memory bank is updated at each batch.

Overall Objective Function and Inference Details

By integrating the aforementioned losses, the overall objective function of target adaptation can be formulated as:

$$\mathcal{L}_{tar} = \mathcal{L}_{ali} + \alpha \mathcal{L}_{pse}, \tag{10}$$

where $\alpha > 0$ is a trade-off parameter. Since we set the pseudo-labels of unknown samples to a uniform distribution, the trained model will output high uncertainty for unknown samples. Therefore, during the inference stage, the separation of known and unknown samples can be achieved by setting a pre-defined uncertainty threshold γ. This process can be represented as:

$$y(x^t) = \begin{cases} \arg\max_c(\delta_c(h(f(x^t)))), & \text{if } E(x^t) < \gamma \\ \text{unknown}, & \text{if } E(x^t) \geq \gamma \end{cases} \tag{11}$$

where $E(x^t)$ denotes the Shannon Entropy (Shannon 1948) of the model's output for sample x^t. We empirically set γ to 0.55 in all experiments which is consistent with previous literature (Qu et al. 2023, 2024).

Experiments

Experimental Setup

Datasets. We conducted a comprehensive evaluation of DTDE on the following DA benchmarks. (1) **Office-31** (Saenko et al. 2010) is a popular small-scale dataset which includes 4,652 images across 31 categories of office items. (2) **Office-Home** (Venkateswara et al. 2017) is a widely recognized medium-scale benchmark, including 65 categories (15,500 images) across four domains: Artistic images (Ar), Clip-Art images (Cl), Product images (Pr), and Real-World images (Rw). (3) **VisDA** (Peng et al. 2017) is a challenging large-scale dataset. The source domain contains 152,397 synthetic images, while the target domain consists of 55,388 real-world images.

Evaluation Protocols and Baselines. In accordance with the main OSDA stream (Pan et al. 2020; Jing, Liu, and Ding 2021; Zhong et al. 2021), we use the average class accuracy over known classes (OS*), the accuracy of unknown class (UNK), and the harmonic mean of OS* and UNK (HOS $= 2\frac{\text{OS}*\times\text{UNK}}{\text{OS}*+\text{UNK}}$) for evaluation. Note that HOS is the most important as it necessitates reliable performance on both known and unknown classes. We omit the details of OS* and it can be found in the appendix. We evaluated DTDE in both the OSDA and the extended UniDA scenarios and the class split is the same with previous works (Saito and Saenko 2021; Qu et al. 2023). For brevity, the class split is illustrated in the form of $(\mathcal{Y}, \overline{\mathcal{Y}}_s, \overline{\mathcal{Y}}_t)$, where $\mathcal{Y}$, $\overline{\mathcal{Y}}_s$, and $\overline{\mathcal{Y}}_t$ denote the number of shared categories, source domain private categories, and target domain unknown categories, respectively. In OSDA settings, we compare the conventional OSDA methods inculding STA (Liu et al. 2019), OSLPP (Wang, Meng, and Breckon 2022), ROS (Bucci, Loghmani, and Tommasi 2020) and ANNA (Li et al. 2023) and the source-free UniDA methods SHOT-O (Liang, Hu, and Feng 2020), GLC (Qu et al. 2023) and LEAD (Qu et al. 2024). Similarly, we also compare the source-accessible methods UAN (You et al. 2019a), CMU (Fu et al. 2020), DCC (Li et al. 2021), OVANet (Saito and Saenko 2021), GATE (Chen et al. 2022) and source free UniDA methods SHOT-O, GLC and LEAD in UniDA setting.

Implementation Details. We employ the most common network architecture in the existing OSDA literature. In particular, we employ the pre-trained ResNet-50 (He et al. 2016) model trained on ImageNet (Deng et al. 2009) as the backbone for all datasets. The batch size is set to 32 in OSDA and 64 in UniDA to be consistent with previous works. The network is optimized using the Stochastic Gradient Descent (SGD) optimizer (Bottou 2010) with a momentum of 0.9. The learning rate is set to 1e-3 for Office-31 and Office-Home, and 1e-4 for VisDA. Deep Embedded Validation (You et al. 2019b) is conducted for hyper-parameters selection. For constant hyper-parameters, we set ϵ to 0.875, and t to 10 in all experiments. The elbow criterion is used

Method	SF	Office-31														Office-Home		VisDA	
		A2D		A2W		D2A		D2W		W2A		W2D		Avg		Avg		S2R	
		UNK	**H**	UNK	**H**	UNK	**H**	UNK	**H**	UNK	**H**	UNK	**H**	UNK	**H**	UNK	**H**	UNK	**H**
STA	✗	45.5	61.6	58.0	71.0	55.0	69.4	49.7	65.5	46.2	60.9	48.5	64.4	50.5	65.5	62.6	61.9	82.4	71.0
OSLPP	✗	90.4	**91.5**	88.4	89.0	76.6	79.3	88.0	92.3	78.5	78.7	91.5	93.6	85.6	87.4	71.7	67.0	65.9	67.1
ROS	✗	77.8	82.4	76.7	82.1	81.2	77.9	93.0	96.0	86.6	77.2	99.4	**99.7**	85.8	85.9	72.4	66.2	73.1	69.0
ANNA	✗	76.1	83.8	88.4	85.5	**91.1**	82.5	**99.6**	**99.5**	87.9	81.6	96.8	98.4	90.0	88.6	76.7	**70.7**	76.1	72.5
SHOT-O	✓	79.2	79.6	80.2	76.5	75.8	78.4	71.5	75.2	83.6	79.3	65.2	73.8	75.9	76.8	40.4	46.0	25.6	28.1
GLC	✓	91.2	86.1	89.8	75.2	89.2	90.5	99.2	89.1	88.0	**90.9**	99.4	96.2	92.8	88.0	76.6	68.2	78.4	71.7
LEAD	✓	91.5	84.2	89.2	81.6	89.5	**90.8**	**99.6**	90.5	87.6	90.0	**99.6**	96.0	93.5	88.9	76.8	68.5	78.0	72.8
DTDE	✓	**98.1**	89.8	**92.7**	**89.4**	89.0	90.2	98.4	93.3	**88.6**	89.8	98.7	95.7	**94.3**	**91.4**	**79.8**	70.3	**84.9**	**80.4**

Table 1: UNK and HOS (H) socres (%) in OSDA scenario on Office-31 (10/0/11), Office-Home (25/0/40) and VisDA (6/0/6). SF indicates source-free adaptation. Some results are cited from ANNA (Li et al. 2023). The results of SHOT-O (Liang, Hu, and Feng 2020), GLC (Qu et al. 2023), and LEAD (based on GLC) (Qu et al. 2024) is from their released code with a batch size of 32 for fair comparison.

Method	SF	Office-Home													Office-31	VisDA
		Ar2Cl	Ar2Pr	Ar2Re	Cl2Ar	Cl2Pr	Cl2Re	Pr2Ar	Pr2Cl	Pr2Re	Re2Ar	Re2Cl	Re2Pr	Avg	Avg	S2R
UAN	✗	51.6	51.7	54.3	61.7	57.6	61.9	50.4	47.6	61.5	62.9	52.6	65.2	56.6	63.5	34.8
CMU	✗	56.0	56.9	59.2	67.0	64.3	67.8	54.7	51.1	66.4	68.2	57.9	69.7	61.6	73.1	32.9
DCC	✗	58.0	54.1	58.0	74.6	70.6	77.5	64.3	73.6	74.9	81.0	75.1	80.4	70.2	80.2	43.0
OVANet	✗	62.8	75.6	78.6	70.7	68.8	75.0	71.3	58.6	80.5	76.1	64.1	78.9	71.8	86.5	53.1
GATE	✗	63.8	75.9	81.4	74.0	72.1	79.8	74.7	70.3	82.7	79.1	71.5	81.7	75.6	87.6	56.4
SHOT-O	✓	32.9	29.5	39.6	56.8	30.1	41.1	54.9	35.4	42.3	58.5	33.5	33.3	40.7	75.0	44.0
GLC	✓	64.3	78.2	**89.8**	63.1	**81.7**	**89.1**	**77.6**	54.2	**88.9**	**80.7**	54.2	**85.9**	75.6	87.8	73.1
LEAD	✓	**65.7**	**79.7**	88.7	65.0	80.3	88.5	**77.6**	57.4	**88.9**	78.9	57.8	85.5	76.2	88.3	76.8
DTDE	✓	62.9	77.6	86.2	**75.8**	77.8	86.4	75.9	**65.5**	86.1	78.6	**62.7**	83.2	**76.6**	**88.6**	**79.4**

Table 2: HOS-score (%) comparison in UniDA scenario on Office-Home (10/5/50), Office-31 (10/10/11) and VisDA (6/3/3) benchmarks. SF indicates source-free adaptation. Some results are cited from LEAD (Qu et al. 2024).

to automatically set the value of λ, which will be discussed in the appendix. The only hyper-parameter that needs to be adjusted in application is α, which is set to 0.3 for Office-31 and VisDA and 1.5 for Office-Home. All experiments are conducted on an RTX-3090 GPU with PyTorch-2.1.0.

Experimental Results

Open-Set Domain Adaptation Evaluation. From Table 1, it can be seen that our method achieves state-of-the-art performance on Offce-31 and VisDA datasets even without accessing source domain data. On Office-Home, the HOS-score of DTDE is comparable to that of ANNA, while the UNK-score is the highest, surpassing ANNA by 3.1%. Notably, the superiority of our method is primarily reflected in the accuracy of the unknown class, as DTDE achieves the highest UNK-score in all threee datasets. This is because previous methods simulate the distribution of unknown samples with source data, whereas our method constructs multiple prototypes through the clustering distributions of the target domain. The clustering distributions over the target domain can better align with the multiple unknown categories of the target domain. the performance of GLC and its variant LEAD is also impressive in the source-free setting, but its one-vs-all global clustering algorithm incurs significant computational overhead. In contrast, the execution time of DTDE is only a fraction or even a tenth of GLC's, which will be demonstrated in the appendix. It is noted that on Visda, DTDE achieves the HOS-score of 80.4%, surpassing our best competitor by a wide margin (7.6%).

Universal Domain Adaptation Evaluation. To further validate the universality of the proposed method, we conduct experiments in the extended UniDA scenario with no modification in the method and report the HOS-score following previous works (You et al. 2019a; Fu et al. 2020; Li et al. 2021; Saito and Saenko 2021; Qu et al. 2023). The comparison results are presented in Table 2. DTDE continues to exhibit advantageous performance on the most challenging VisDA dataset with the highest HOS-score of 79.4%. On all three datasets, even though DTDE does not have a specific treatment for source private categories compared to the UniDA methods, it still achieves the best performance.

Method	Office-31		Office-Home		VisDA	
	UNK	**HOS**	UNK	**HOS**	UNK	**HOS**
Source model	91.4	67.8	62.1	58.0	72.4	29.3
Ours (w/o $\mathcal{L}_{pse}$)	93.4	87.3	65.3	61.5	64.1	63.2
Ours (w/o $\mathcal{L}_{ali}$)	**94.7**	88.2	76.3	65.4	83.1	75.6
Ours (w/o w)	94.2	90.8	79.5	69.3	84.2	79.8
Ours (w/o ϵ)	79.5	89.6	79.5	68.9	83.8	78.2
Ours (full)	94.3	**91.4**	**79.8**	**70.3**	**84.9**	**80.4**

Table 3: Ablation Studies. Results for OSDA on Office-31, Office-Home, and VisDA with different variants of DTDE.

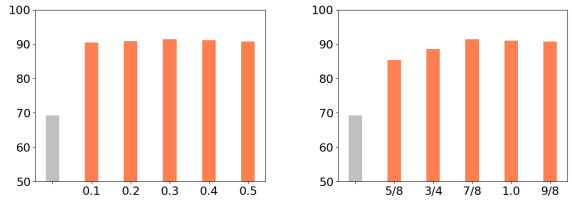

(a) HOS-score with varying α (b) HOS-score with varying ϵ

Figure 2: Hyper-parameter Sensitivity Analysis. On Office-31, the HOS-score is shown as the values of the involved hyper-parameters vary. Note that when varying the value of a particular hyper-parameter, the other parameters are fixed at their optimal values.

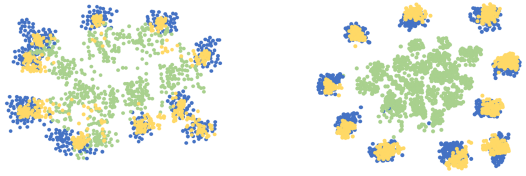

(a) Source model (b) DTDE

Figure 3: Visualization of Features after Training. OSDA task D→A is performed on Office-31. The yellow, blue, and green points respectively represent source samples, known target samples, and unknown target samples.

Analytical Experiments

Ablation Studies. As shown in Table 3, we conducted ablation experiments on four variants of DTDE across the three datasets. It can be concluded that $\mathcal{L}_{pse}$ is quite effective in identifying unknown samples, as the UNK-score experience a decrease compared to the source model across all three datasets in its absence (0.9% on Office-31, 14.5% on Office-Home, and 20.8% on VisDA). This is because if unknown samples are not accurately identified, the overconfidence problem can lead to a large number of unknown samples being incorrectly identified as known samples. $\mathcal{L}_{ali}$ mainly improves the accuracy of known class (OS*-score) since it can offset the negative impacts of the incorrect pseudo-labels based on the nearest neighbors. Moreover, our class weight w and adaptive sampling parameter ϵ both contribute to further improvements in experimental performance.

Hyper-parameter Sensitivity Analysis. We studied the parameter sensitivity of DTDE on Office-31 in OSDA and present the results in Figure 2. It can be observed that varying α has little impact on the experimental results. $\epsilon = 0.875$ is appropriate because a large value will decrease the prototype quality, while a small value will compromise the prototype diversity. Generally, our method is relatively stable across different parameters.

Visualization of Clustering Self-splitting Mechanism. As the evaluation of clustering distribution in the target domain is crucial in our method to identify the distribution of unknown samples, we illustrate the clustering self-splitting process through t-SNE visualization in Figure 4. In the first iteration with only three clusters, it is evident that samples from known and unknown categories are entirely mixed together. As the number of iterations increases, the known and unknown samples start to gradually separate. After the final iteration, it is clear to distinguish which clusters belonged to the known samples and which belonged to the unknown samples. This phenomenon indicates that the samples in the target domain does exhibit a clustering distribution.

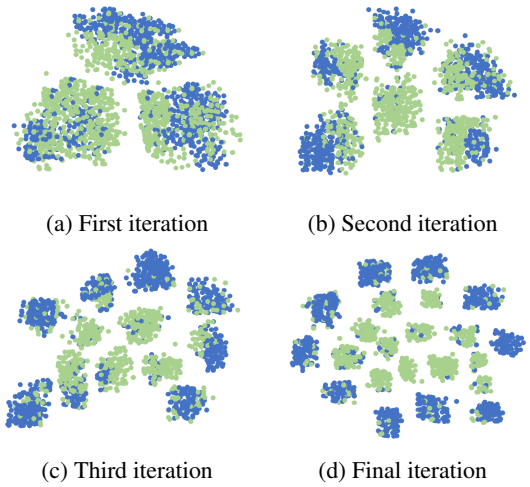

(a) First iteration (b) Second iteration

(c) Third iteration (d) Final iteration

Figure 4: Visualization of Clustering Self-splitting Mechanism. OSDA task A→D is performed on Office-31. Blue and green points are respectively features of known and unknown classes.

Visualization of Features after Training. As shown in Figure 3, we conducted T-SNE feature comparisons of the source model and the proposed DTDE. The feature distribution of the source model is scattered, and the boundary between known and unknown samples is ambiguous. Furthermore, it can be roughly observed that samples from unknown categories also exhibit some clustered distributions. In contrast, our method shows a more compact clustering of known samples, and the unknown samples also exhibit clear clustering distributions away from the known samples.

Conclusion

In this paper, we analyze the issues of unavailable source data and semantic inconsistencies that may arise in unsupervised domain adaptation. To tackle these, we propose a novel Dynamic Target Distribution Estimation (DTDE) method, which attempts to identify known and unknown sample clustering distributions in the unlabeled target domain for prototype construction. We propose a novel self-splitting strategy for target clustering estimation. A class-aware k-nearest neighbors alignment method further improves pseudo-label accuracy, particularly for challenging categories. Comprehensive evaluations demonstrate DTDE's effectiveness, achieving a notable 7.6% performance improvement over the best competitor on the VisDA benchmark.

Acknowledgments

This work was supported in part by the National Natural Science Foundation of China under Grant 62176042, in part by TCL Technology Innovation Funding SS2024105, in part by the Fundamental Research Funds for the Central Universities (UESTC) under Grant ZYGX2024Z008, and in part by Tencent Marketing Solution Rhino-Bird Focused Research Program.

References

Achituve, I.; Maron, H.; and Chechik, G. 2021. Self-supervised learning for domain adaptation on point clouds. In *Proceedings of the IEEE/CVF winter conference on applications of computer vision*, 123–133.

Bottou, L. 2010. Large-scale machine learning with stochastic gradient descent. In *Proceedings of COMPSTAT'2010: 19th International Conference on Computational StatisticsParis France, August 22-27, 2010 Keynote, Invited and Contributed Papers*, 177–186. Springer.

Bucci, S.; D'Innocente, A.; Liao, Y.; Carlucci, F. M.; Caputo, B.; and Tommasi, T. 2021. Self-supervised learning across domains. *IEEE Transactions on Pattern Analysis and Machine Intelligence*, 44(9): 5516–5528.

Bucci, S.; Loghmani, M. R.; and Tommasi, T. 2020. On the effectiveness of image rotation for open set domain adaptation. In *European conference on computer vision*, 422–438. Springer.

Chen, C.; Xie, W.; Huang, W.; Rong, Y.; Ding, X.; Huang, Y.; Xu, T.; and Huang, J. 2019. Progressive feature alignment for unsupervised domain adaptation. In *Proceedings of the IEEE/CVF conference on computer vision and pattern recognition*, 627–636.

Chen, L.; Lou, Y.; He, J.; Bai, T.; and Deng, M. 2022. Geometric anchor correspondence mining with uncertainty modeling for universal domain adaptation. In *Proceedings of the IEEE/CVF Conference on Computer Vision and Pattern Recognition*, 16134–16143.

Deng, J.; Dong, W.; Socher, R.; Li, L.-J.; Li, K.; and Fei-Fei, L. 2009. Imagenet: A large-scale hierarchical image database. In *2009 IEEE conference on computer vision and pattern recognition*, 248–255. Ieee.

Ding, N.; Xu, Y.; Tang, Y.; Xu, C.; Wang, Y.; and Tao, D. 2022. Source-free domain adaptation via distribution estimation. In *Proceedings of the IEEE/CVF Conference on Computer Vision and Pattern Recognition*, 7212–7222.

Fu, B.; Cao, Z.; Long, M.; and Wang, J. 2020. Learning to detect open classes for universal domain adaptation. In *Computer Vision–ECCV 2020: 16th European Conference, Glasgow, UK, August 23–28, 2020, Proceedings, Part XV 16*, 567–583. Springer.

Ganin, Y.; and Lempitsky, V. 2015. Unsupervised domain adaptation by backpropagation. In *International conference on machine learning*, 1180–1189. PMLR.

Ganin, Y.; Ustinova, E.; Ajakan, H.; Germain, P.; Larochelle, H.; Laviolette, F.; March, M.; and Lempitsky, V. 2016. Domain-adversarial training of neural networks. *Journal of machine learning research*, 17(59): 1–35.

Goodfellow, I.; Pouget-Abadie, J.; Mirza, M.; Xu, B.; Warde-Farley, D.; Ozair, S.; Courville, A.; and Bengio, Y. 2014. Generative adversarial nets. *Advances in neural information processing systems*, 27.

Gu, X.; Sun, J.; and Xu, Z. 2020. Spherical space domain adaptation with robust pseudo-label loss. In *Proceedings of the IEEE/CVF conference on computer vision and pattern recognition*, 9101–9110.

He, K.; Zhang, X.; Ren, S.; and Sun, J. 2016. Deep residual learning for image recognition. In *Proceedings of the IEEE conference on computer vision and pattern recognition*, 770–778.

Hoffman, J.; Tzeng, E.; Park, T.; Zhu, J.-Y.; Isola, P.; Saenko, K.; Efros, A.; and Darrell, T. 2018. Cycada: Cycle-consistent adversarial domain adaptation. In *International conference on machine learning*, 1989–1998. Pmlr.

Jang, J.; Na, B.; Shin, D. H.; Ji, M.; Song, K.; and Moon, I.-C. 2022. Unknown-aware domain adversarial learning for open-set domain adaptation. *Advances in Neural Information Processing Systems*, 35: 16755–16767.

Jiang, L.; Meng, D.; Yu, S.-I.; Lan, Z.; Shan, S.; and Hauptmann, A. 2014. Self-paced learning with diversity. *Advances in neural information processing systems*, 27.

Jing, T.; Liu, H.; and Ding, Z. 2021. Towards novel target discovery through open-set domain adaptation. In *Proceedings of the IEEE/CVF International Conference on Computer Vision*, 9322–9331.

Kang, G.; Jiang, L.; Yang, Y.; and Hauptmann, A. G. 2019. Contrastive adaptation network for unsupervised domain adaptation. In *CVPR*, 4893–4902.

Li, G.; Kang, G.; Zhu, Y.; Wei, Y.; and Yang, Y. 2021. Domain consensus clustering for universal domain adaptation. In *Proceedings of the IEEE/CVF conference on computer vision and pattern recognition*, 9757–9766.

Li, W.; Liu, J.; Han, B.; and Yuan, Y. 2023. Adjustment and Alignment for Unbiased Open Set Domain Adaptation. In *Proceedings of the IEEE/CVF Conference on Computer Vision and Pattern Recognition*, 24110–24119.

Liang, J.; Hu, D.; and Feng, J. 2020. Do we really need to access the source data? source hypothesis transfer for unsupervised domain adaptation. In *International conference on machine learning*, 6028–6039. PMLR.

Liu, H.; Cao, Z.; Long, M.; Wang, J.; and Yang, Q. 2019. Separate to adapt: Open set domain adaptation via progressive separation. In *Proceedings of the IEEE/CVF conference on computer vision and pattern recognition*, 2927–2936.

Liu, H.; Wang, J.; and Long, M. 2021. Cycle self-training for domain adaptation. *Advances in Neural Information Processing Systems*, 34: 22968–22981.

Liu, Y.; Zhang, W.; and Wang, J. 2021. Source-free domain adaptation for semantic segmentation. In *Proceedings of the IEEE/CVF Conference on Computer Vision and Pattern Recognition*, 1215–1224.

Long, M.; Cao, Y.; Wang, J.; and Jordan, M. 2015. Learning transferable features with deep adaptation networks. In *International conference on machine learning*, 97–105. PMLR.

Long, M.; Zhu, H.; Wang, J.; and Jordan, M. I. 2017. Deep transfer learning with joint adaptation networks. In *ICML*, 2208–2217. PMLR.

Lu, Y.; Shen, M.; Ma, A. J.; Xie, X.; and Lai, J.-H. 2023. MLNet: Mutual Learning Network with Neighborhood Invariance for Universal Domain Adaptation. *arXiv preprint arXiv:2312.07871*.

Luo, Y.; Wang, Z.; Huang, Z.; and Baktashmotlagh, M. 2020. Progressive graph learning for open-set domain adaptation. In *International Conference on Machine Learning*, 6468–6478. PMLR.

Ma, N.; Bu, J.; Lu, L.; Wen, J.; Zhou, S.; Zhang, Z.; Gu, J.; Li, H.; and Yan, X. 2022. Context-guided entropy minimization for semi-supervised domain adaptation. *Neural Networks*, 154: 270–282.

MacQueen, J.; et al. 1967. Some methods for classification and analysis of multivariate observations. In *Proceedings of the fifth Berkeley symposium on mathematical statistics and probability*, 14, 281–297. Oakland, CA, USA.

Pan, Y.; Yao, T.; Li, Y.; Ngo, C.-W.; and Mei, T. 2020. Exploring category-agnostic clusters for open-set domain adaptation. In *Proceedings of the IEEE/CVF conference on computer vision and pattern recognition*, 13867–13875.

Panareda Busto, P.; and Gall, J. 2017. Open set domain adaptation. In *Proceedings of the IEEE international conference on computer vision*, 754–763.

Peng, X.; Usman, B.; Kaushik, N.; Hoffman, J.; Wang, D.; and Saenko, K. 2017. Visda: The visual domain adaptation challenge. *arXiv preprint arXiv:1710.06924*.

Qu, S.; Zou, T.; He, L.; Röhrbein, F.; Knoll, A.; Chen, G.; and Jiang, C. 2024. Lead: Learning decomposition for source-free universal domain adaptation. In *Proceedings of the IEEE/CVF Conference on Computer Vision and Pattern Recognition*, 23334–23343.

Qu, S.; Zou, T.; Röhrbein, F.; Lu, C.; Chen, G.; Tao, D.; and Jiang, C. 2023. Upcycling models under domain and category shift. In *Proceedings of the IEEE/CVF Conference on Computer Vision and Pattern Recognition*, 20019–20028.

Saenko, K.; Kulis, B.; Fritz, M.; and Darrell, T. 2010. Adapting visual category models to new domains. In *Computer Vision–ECCV 2010: 11th European Conference on Computer Vision, Heraklion, Crete, Greece, September 5-11, 2010, Proceedings, Part IV 11*, 213–226. Springer.

Saito, K.; Kim, D.; Sclaroff, S.; and Saenko, K. 2020. Universal domain adaptation through self supervision. *Advances in neural information processing systems*, 33: 16282–16292.

Saito, K.; and Saenko, K. 2021. Ovanet: One-vs-all network for universal domain adaptation. In *Proceedings of the ieee/cvf international conference on computer vision*, 9000–9009.

Saito, K.; Yamamoto, S.; Ushiku, Y.; and Harada, T. 2018. Open set domain adaptation by backpropagation. In *Proceedings of the European conference on computer vision (ECCV)*, 153–168.

Shannon, C. E. 1948. A mathematical theory of communication. *The Bell system technical journal*, 27(3): 379–423.

Shermin, T.; Lu, G.; Teng, S. W.; Murshed, M.; and Sohel, F. 2020. Adversarial network with multiple classifiers for open set domain adaptation. *IEEE Transactions on Multimedia*, 23: 2732–2744.

Su, W.; Han, Z.; He, R.; Wei, B.; He, X.; and Yin, Y. 2023. Neighborhood-based credibility anchor learning for universal domain adaptation. *Pattern Recognition*, 142: 109686.

Tzeng, E.; Hoffman, J.; Saenko, K.; and Darrell, T. 2017. Adversarial discriminative domain adaptation. In *Proceedings of the IEEE conference on computer vision and pattern recognition*, 7167–7176.

Venkateswara, H.; Eusebio, J.; Chakraborty, S.; and Panchanathan, S. 2017. Deep hashing network for unsupervised domain adaptation. In *Proceedings of the IEEE conference on computer vision and pattern recognition*, 5018–5027.

Wang, Q.; Meng, F.; and Breckon, T. P. 2022. Progressively select and reject pseudo-labelled samples for open-set domain adaptation. In *Proceedings of the AAAI conference on artificial intelligence*.

Xia, H.; Zhao, H.; and Ding, Z. 2021. Adaptive adversarial network for source-free domain adaptation. In *Proceedings of the IEEE/CVF International Conference on Computer Vision*, 9010–9019.

Yang, S.; van de Weijer, J.; Herranz, L.; Jui, S.; et al. 2021. Exploiting the intrinsic neighborhood structure for source-free domain adaptation. *Advances in neural information processing systems*, 34: 29393–29405.

You, K.; Long, M.; Cao, Z.; Wang, J.; and Jordan, M. I. 2019a. Universal domain adaptation. In *Proceedings of the IEEE/CVF conference on computer vision and pattern recognition*, 2720–2729.

You, K.; Wang, X.; Long, M.; and Jordan, M. 2019b. Towards accurate model selection in deep unsupervised domain adaptation. In *International Conference on Machine Learning*, 7124–7133. PMLR.

Yu, Z.; Li, J.; Zhu, L.; Lu, K.; and Shen, H. T. 2022. Uneven Bi-Classifier Learning for Domain Adaptation. *IEEE Transactions on Circuits and Systems for Video Technology*.

Yu, Z.; Li, J.; Zhu, L.; Lu, K.; and Shen, H. T. 2023. Classification Certainty Maximization for Unsupervised Domain Adaptation. *IEEE Transactions on Circuits and Systems for Video Technology*.

Zhong, L.; Fang, Z.; Liu, F.; Yuan, B.; Zhang, G.; and Lu, J. 2021. Bridging the theoretical bound and deep algorithms for open set domain adaptation. *IEEE transactions on neural networks and learning systems*.